Pediatr Radiol (2014) 44:713–718
DOI 10.1007/s00247-014-2886-3

ORIGINAL ARTICLE

Hepatic involvement of Langerhans cell histiocytosis in children—imaging findings of computed tomography, magnetic resonance imaging and magnetic resonance cholangiopancreatography

Yingyan Shi · Zhongwei Qiao · Chunmei Xia · Ying Gong · Haowei Yang · Guoping Li · Mier Pa

Received: 31 July 2013 / Revised: 22 November 2013 / Accepted: 17 January 2014 / Published online: 28 February 2014

Abstract
Background Langerhans cell histiocytosis is a rare disease that occurs mainly in children, and hepatic involvement is generally a poor prognostic factor.
Objective To describe CT and MRI findings of hepatic involvement of Langerhans cell histiocytosis in children, especially the abnormal bile duct manifestation on magnetic resonance cholangiopancreatography (MRCP).
Materials and methods Thirteen children (seven boys, six girls; mean age 28.9 months) were diagnosed with disseminated Langerhans cell histiocytosis. They underwent CT (n=5) or MRI (n=4), or CT and MRI examinations (n=4) to evaluate the liver involvement.
Results Periportal abnormalities presented as band-like or nodular lesions on CT and MRI in all 13 children. The hepatic parenchymal lesions were found in the peripheral regions of the liver in seven children, including multiple nodules on MRI (n=6), and cystic-like lesions on CT and MRI (n=3). In 11 of the 13 children the dilatations of the bile ducts were observed on CT and MRI. Eight of the 13 children underwent MR cholangiopancreatography, which demonstrated stenoses or segmental stenoses with slight dilatation of the central bile ducts, including the common hepatic duct and its first-order branches. The peripheral bile ducts in these children showed segmental dilatations and stenoses.
Conclusion Stenosis of the central bile ducts revealed by MR cholangiopancreatography was the most significant finding of liver involvement in Langerhans cell histiocytosis in children.

Keywords Langerhans cell histiocytosis · Hepatic bile duct · Computed tomography · Magnetic resonance imaging · Magnetic resonance cholangiopancreatography · Liver · Children

Y. Shi · Z. Qiao (✉) · Y. Gong · H. Yang · G. Li · M. Pa
Department of Radiology, Children's Hospital of Fudan University,
399 Wanyuan Road, Minhang District,
Shanghai 201102, People's Republic of China
e-mail: zqiao@fudan.edu.cn

C. Xia
Physiology and Pathophysiology Department,
Shanghai Medical College of Fudan University,
130 Dongan Road, Xuhui District,
Shanghai 200032, People's Republic of China

Introduction

Langerhans cell histiocytosis is a rare disease that occurs mainly in children and has a wide clinical spectrum varying from a localized lesion to disseminated lesions [1]. Disseminated Langerhans cell histiocytosis is a life-threatening condition affecting multiple organ systems and usually occurs in infants and young children; hepatic involvement has been recognized as a risk factor with a poor prognosis [2, 3]. Confirming hepatic infiltration in Langerhans cell histiocytosis is significant for planning a treatment strategy and improving the prognosis of patients [4].

Diagnostic imaging plays an important role in visualizing hepatic infiltration in Langerhans cell histiocytosis. Periportal abnormalities demonstrated on US, CT and MRI, though lacking in specificity, have been reported as the most important features of hepatic involvement in Langerhans cell histiocytosis; these abnormalities are related to periportal inflammation and infiltration or fibrosis [5–13]. However, Langerhans cell histiocytosis in the liver causes exquisite tropism of the bile ducts. It has been reported that Langerhans cells mainly affect the major and perihilar bile ducts, consequently leading to cholestasis [14, 15]. Direct infiltration of bile ducts by Langerhans cells has also been reported to be the pathogenesis of Langerhans-induced sclerosing cholangitis, and the CD1a-

positive Langerhans cells have been observed to destroy the walls of major ducts on immunohistochemical staining [13, 15]. Magnetic resonance cholangiopancreatography (MRCP), when imaging the bile within the biliary tree with heavily T2-weighted sequences, might be more sensitive than US, CT and conventional MRI in revealing the bile duct abnormalities [16].

Until now, two cases of bile duct abnormalities have been reported in detail on MRCP in LCH patients [4, 17]. The purpose of this study was to demonstrate CT and MRI findings of hepatic involvement in pediatric Langerhans cell histiocytosis and to highlight our initial observation on the bile duct abnormalities using MRCP in eight young children.

Materials and methods

Patients

This review was approved by the ethics committee of our institution. From April 2008 to June 2012, 51 children were diagnosed at our institution with Langerhans cell histiocytosis. If US imaging of the liver of these patients indicated the abnormality, then an MRI or CT examination followed. Thirteen children underwent CT or MRI or both at the Department of Radiology of our hospital, including seven boys and six girls with a mean age of 28.9 months and range of 13–52 months. Clinically, they were all categorized as having disseminated Langerhans cell histiocytosis. In these children liver involvement is suspected if they have one or more of the following indications: jaundice, elevated liver enzymes, hypoproteinemia and portal hypertension. Eight of the children had elevated serum of hepatic enzymes. Seven manifested jaundice. Three had suspected hepatic lesions during examination, the primary lesions being in the pituitary or bones. One of them did not show obvious hepatic-related symptoms. Two of them had hepatic lesions confirmed 2 weeks to 6 months after being diagnosed with Langerhans cell histiocytosis but without hepatic-related symptoms. The other organs involved by Langerhans cell histiocytosis included skin (n=8), cranial bone (n=4), pituitary (n=2), ilium and rib (n=2). A series of biopsy specimens were obtained from skin, bone and liver of these children for further pathological analysis.

CT and MRI examinations

The imaging examinations in 13 children included CT (n=5) or MRI (n=4), or CT and MRI (n=4) (Table 1). Nine of the 13 children underwent abdominal CT, which included noncontrast- and contrast-enhanced scans with a delay of 60–70 s after initiation of intravenous injection of contrast material (Omnipaque, 300 mg iodine/ml, dose 1.5–2 ml/kg; GE Medical Systems, Milwaukee, WI) at a rate of 1–2 ml/s. All CT examinations were performed on a 64-detector row scanner (LightSpeed, GE Medical Systems) with 50–60 mAs and 100–120 kVp, slice thickness 5 mm. The console-displayed volume CT dose indices ($CTDI_{vol}$, units mGy) ranged 2.56–3.20 mGy, and dose length product (DLP, units mGy-cm) ranged 112.52–127.86 mGy-cm based on the 32-cm body phantom.

Table 1 Demographics of 13 children with hepatic involvement of Langerhans cell histiocytosis

Patient number	Gender	Age (months)	Organs involved	Image modalities
1	F	18	Liver, temporal bone[a]	MRI, MRCP
2	F	36	Pituitary, liver, scalp[a]	MRI, MRCP
3	M	14	Liver[a], skin[a]	MRI, MRCP
4	M	52	Skin[a], liver	MRI, MRCP
5	M	25	Liver, skin[a]	CT, MRI, MRCP
6	F	15	Skin[a], liver	CT, MRI, MRCP
7	M	36	Frontal bone[a], liver[a]	CT, MRI, MRCP
8	F	48	Pituitary, liver[a]	CT, MRCP
9	M	36	Temporal bone[a], liver	CT
10	M	13	Skin[a], blood, liver	CT
11	M	22	Ilium[a], liver	CT
12	F	48	Liver, cranial bones[a], skin, rib	CT
13	F	15	Liver, skin[a]	CT

[a] The biopsy specimens were obtained from these organs. *MRCP* MR cholangiopancreatography

Eight of the 13 children underwent MRI (four had undergone CT prior to MRI) on a 1.5-T system (Avanto; Siemens, Erlangen, Germany) with phased-array body coil. The MR sequences included a fast imaging with steady-state precession (FISP) sequence for a pilot scan, and respiratory-gated turbo spin echo (TSE) T2-weighted imaging (repetition time/echo time [TR/TE] >4,000/102 ms, echo train length [ETL] 25, number of excitations [NEX] 1 and slice thickness 5 mm); respiratory-gated turbo fast low angle shot (FLASH) T1-weighted imaging (TR/TE >1,540 ms/2.3 ms, inversion time [TI] 900 ms, flip angle 15°, NEX 2); enhanced T1-weighted imaging was performed in two children after administration of contrast medium (Omniscan, GE Healthcare Ireland, Cork, Ireland) at a dose of 0.1 mmol/kg.

Eight children underwent MRCP with respiratory-gated 3-D heavily T2-weighted imaging plus fat saturation. The parameters included TR/TE >4,000 ms/714 ms, ETL 115, slice thickness 1 mm and NEX 2. Maximum-intensity projection and multi-planar reformatted images on raw data were obtained on an MR workstation (Syngo, version MR B17; Siemens, Erlangen, Germany).

CT and MRI data analysis

CT and MRI datasets were reviewed on the PACS and MRI workstations by two radiologists with more than 9 years of experience with CT and MR imaging. The radiologists were

blinded to the clinical information and a consensus interpretation of image findings was performed in cases of discordance.

CT and MRI were analyzed according to the following criteria: (1) the periportal lesion distribution. Central periportal lesion was described when it presented along the main portal vein and its first-order branches, and peripheral periportal lesion was described when it presented along the distal portal vein branches [18]; (2) the density/signal intensity of periportal lesions on CT and MRI (defined as hypo-, iso- or hyper-dense signal intensity compared with normal liver parenchyma); (3) enhancement patterns of periportal lesions on CT and MRI, and enhancement degrees on CT, which were defined as mild (less than 30 Hounsfield units [HU]), moderate (30–60 HU) or remarkable (more than 60 HU) enhancement; (4) bile duct abnormalities on CT, MRI and MRCP images. Bile duct dilatation was evaluated on contrast-enhanced CT and T2-W MR images, and the bile duct dilatations and stenoses were evaluated on MRCP. We defined the central bile duct as the common hepatic duct and its first-order branches, and the peripheral bile duct as the bile duct distal to the first-order branches. The biliary stenoses and dilatations were defined in comparison with their neighboring ducts. Ductal dilatation was considered present if the diameter of the bile duct was greater than that of the central portion [16]. The type of dilatation was described as cylindrical, cystic or a bead-like pattern.

Pathology

All the biopsy specimens obtained from skin, bone and liver of the children were identified by using hematoxylin-eosin and immunohistochemical staining (Langerhans cell markers such as CD1a, CD68, langerin and S-100 protein) by the pathologists at our institution.

Results

The imaging findings of hepatic abnormalities in Langerhans cell histiocytosis on CT, MRI and MRCP are summarized in Table 2.

Bile duct abnormalities

The bile duct abnormalities were found on contrast-enhanced CT, T2-W MRI and MRCP images. Dilatation of the intrahepatic bile ducts in 11 of the 13 children presented as hypodensity on contrast-enhanced CT and hyperintensity on T2-W MRI and MRCP images (Table 2). Eight children underwent MRCP, and five of them showed stenoses of the central bile duct manifesting as the interruption of the common hepatic duct and its first-order branches, and three of them showed segmental stenoses with slight dilatations of those major bile ducts (Figs. 1, 2 and 3). Furthermore, we observed segmental stenoses and dilatations of the peripheral bile ducts in both the right and left lobes in these eight children. The dilatation of the peripheral bile ducts was seen on MRCP as a cylindrical pattern in 3/8, a cystic pattern in 2/8 and a beading pattern in 6/8.

Periportal abnormal density/signal intensity

The periportal abnormalities were present as band-like or nodular lesions on CT and MRI in all patients. These lesions were distributed along the portal vein trees in the left and right lobes and were mainly hypodense on noncontrast CT (8/9) (Fig. 4) and mixed hypointense and hyperintense signal on T2-W MRI. They showed mixed hypointense and hyperintense signal (5/7) or hypodensity (2/7) on T1-W MRI (Figs. 1 and 2). The periportal lesions were moderately and heterogeneously enhanced after administration of the contrast media (Figs. 2 and 4).

Parenchymal lesions

The hepatic parenchymal lesions were found in the peripheral regions of the liver in seven children, including multiple nodules on MRI (n=6), and cystic-like lesions on CT and MRI (n=3). The diameter of parenchymal lesions ranged 2–20 mm, and they appeared hypointense on T1-W MRI and hyperintense on T2-W MRI. After administration of contrast media, the nodular lesions were homogeneously enhanced and the cystic-like lesions showed ring-like enhancement on CT (Fig. 3).

Table 2 CT and MRI findings in 13 children with hepatic involvement of Langerhans cell histiocytosis

CT/MRI findings		Plain CT	CECT	T1-W MRI	T2-W MRI	MRCP
Intrahepatic bile ducts	Dilatation		7/9		6/7	Bead-type pattern 6/8 Cylindrical 3/8 Cystic 2/8
	Stenosis					8/8
Periportal lesions	Hypo-density/-intensity	8/9	Moderate enhancement (9/9)	2/7	0	
	Mixed density/-intensity	1/9		5/7	7/7	
Parenchymal lesions	Nodular lesions		0	6/7	6/7	
	Cystic-like lesions		2/9	0	1/7	

CECT contrast-enhanced computed tomography, *MRCP* MR cholangiopancreatography

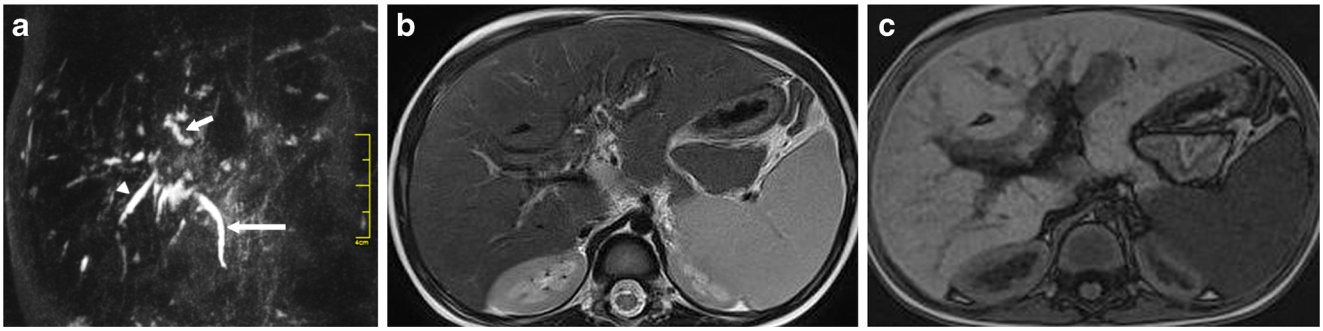

Fig. 1 MRCP and MRI in a 25-month-old boy (patient 5). **a** MRCP image demonstrates total interruption of the common hepatic duct and its first-order branches. Segmental dilatation of the peripheral bile ducts in both the left and right lobes can be seen. Note the common bile duct (*long arrow*), the left hepatic duct branch (*short arrow*) and the right hepatic duct branch (*arrowhead*). **b** The periportal lesions show slightly heterogeneous signal intensity on axial T2-W MR image. The dilated left bile duct shows high signal intensity, surrounded by the lower-intensity periportal lesions. **c** The periportal lesions show mainly low intensity with patchy high intensity on axial T1-W MR image. *MRCP* magnetic resonance cholangiopancreatography

Liver pathology

Biopsy of the liver was performed in three children (patients 3, 7 and 8 in Table 1). In patients 3 and 7, ductular proliferation and fibrosis was observed on histopathology.

In patient 8 there was infiltration of histiocytic and inflammatory cells, and cystic changes (based on the inflammatory nodules with central eosinophils and peripheral Langerhans cells) were observed on histopathology, and the Langerhans markers, e.g., CD1a, S-100 protein and langerin (CD207), were positive in these lesions on immunohistochemical staining. The multiple cystic lesions in this child were identified on CT (Fig. 3), while MRCP imaging demonstrated the stenoses of the common hepatic duct and its first-order branches, with segmental dilatations of the left large bile duct, slight dilatations of the peripheral small bile ducts and multiple cystic lesions along the biliary system.

Discussion

In the liver Langerhans cells show an unusual affinity to the bile ducts [15]. The association between Langerhans cell histiocytosis and sclerosing cholangitis has been well established [13, 19]. It has been reported that Langerhans cells mainly involve the major and perihilar bile ducts [14]. The preferential involvement of the major bile ducts also explains why Langerhans infiltration is so rarely found on the percutaneous biopsy of the liver [15]. Therefore it is important to detect the hepatic lesions in Langerhans cell histiocytosis by using image modalities such as US, CT and MRI. MRCP has been found to

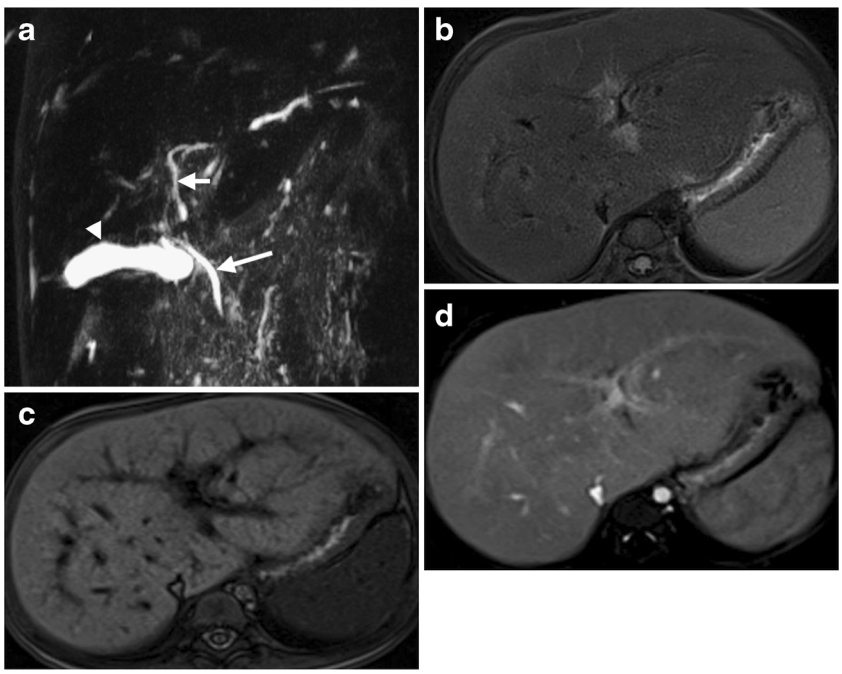

Fig. 2 MRCP and MRI in a 15-month-old girl (patient 6). **a** MRCP image demonstrates multiple stenoses of the common hepatic duct and its first-order branches. Segmental dilatations and stenoses of the left hepatic duct branch can be seen. The right hepatic duct branch was not seen on MRCP. The normal common bile duct is noted (*long arrow*), along with the left hepatic duct branch (*short arrow*) and the gallbladder (*arrowhead*). **b** The central periportal lesion demonstrates mainly high signal intensity on axial T2-W MRI and low signal intensity on (**c**) axial T1-W MRI, and moderate enhancement on (**d**) contrast-enhanced axial T1-W MRI. *MRCP* magnetic resonance cholangiopancreatography

Fig. 3 MRCP and CT in a 4-year-old girl (patient 8). **a** MRCP demonstrates multiple dilatations and stenoses of the common hepatic duct and its branches. Multiple cystic-like lesions along the intrahepatic biliary system can be seen, and there is a large gallbladder. Note the common bile duct (*long arrow*), the left hepatic duct branch (*short arrow*) and the right hepatic duct branch (*arrowhead*). **b** Nonenhanced axial CT shows multiple hypodense cystic lesions. **c** On contrast-enhanced axial CT there is ring-like enhancement of the lesions. *MRCP* magnetic resonance cholangiopancreatography

be more sensitive than US, CT and conventional MRI in revealing the bile duct abnormalities in Langerhans-induced sclerosing cholangitis, and its diagnostic accuracy was comparable to that of endoscopic retrograde cholangiopancreatography [16, 20].

In the current study, the significant findings on MRCP images were multiple stenoses and segmental dilatations of the central and peripheral bile ducts. With respect to the central bile ducts the interruption of the common hepatic duct and its first-order branches was the most characteristic finding on MRCP, consistent with the report that the major and the perihilar bile ducts were the ones mainly affected by Langerhans cells [14]. Furthermore, concerning the peripheral bile ducts, cylindrical or cystic dilatation and a bead-like pattern of biliary branches were manifested in the left and right lobes, consistent with the previous observations on both radiologic imaging and pathological detection [13, 14]. The findings of normal appearance of the extrahepatic bile ducts and segmental dilatations and stenoses of the intrahepatic bile duct branches were consistent with the characteristic manifestation of sclerosing cholangitis [14, 17].

The multiple stenoses and long-segmental interruption of the bile ducts might be attributed to the proliferation of ductal walls [8, 13]. On pathology, Langerhans cells were present within the basement membrane of the bile ducts, stripping the residual epithelial cells off the ductal wall [13, 15]. Infiltration by Langerhans cells, inflammatory cells or proliferation of ductal walls could lead to the multiple stenoses and long-segmental interruption of the bile ducts [8, 13], while the dilatation of bile ducts might be the secondary offset to the proximal bile duct stenosis, or the direct sequel of the destructive cholangitis [13]. In fact, we observed that the stenoses of the bile ducts were in line with periportal lesions on axial CT and MRI. Therefore the stenoses of the central bile ducts on MRCP were underlying the extensive periportal lesions in the perihilar area demonstrated on T1- and T2-W MRI.

The varied CT and MRI findings of periportal lesions in our study have been reported [5, 8–11]. In the seven children who had MRI the periportal lesions manifested as heterogeneous signal intensity on T1-W and T2-W images, implicating the pathological evolution of hepatic Langerhans cell histiocytosis. It has been reported that in the proliferative and granulomatous stage, periportal lesions are hypodense on CT, hypointense on T1-W MR and hyperintense on T2-W MRI; in the xanthomatous stage, because of periportal fatty infiltration, the lesions appeared hypodense on CT images and hyperintense on T1-W MRI; in the fibrous stage, hypo-signal intensity on T2-W MR and spotty calcification on CT might be presented [1, 7, 10, 11]. The heterogeneous signal intensity pattern in our patients was possibly caused by the coexistence of mixed pathological conditions, such as inflammation, fat infiltration and fibrosis [13].

Multiple nodular and cystic-like lesions in the peripheral regions of the liver were observed in our study. The scattered and well-defined nodular lesions appeared hypodense on plain

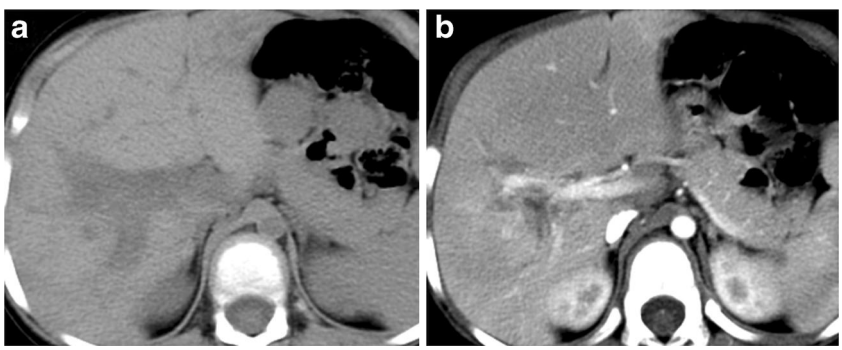

Fig. 4 Periportal lesions on axial CT in a 3-year-old boy (patient 9). **a** The periportal lesions are hypodense on noncontrast axial CT. **b** After administration of contrast agent, the periportal lesions are moderately enhanced

CT, hypointense on T1-W MRI and hyperintense on T2-W MRI, and with a homogeneous enhancement pattern after administration of contrast media. Pathologically, the nodular lesions were possibly Langerhans cell infiltrations that produced cell masses ranging from focal granulomatoid foci to confluent tumor-like lesions [13]. In fact, in addition to bile duct proliferation with portal triaditis, the nodular parenchymal lesion with triaditis was one of the common pathological patterns in hepatic involvement by Langerhans cells [21]. Furthermore, the cystic-like lesions demonstrated in our three patients were hypodense on plain CT and hypointense on T1-W MRI and hyperintense on T2-W MR images, with a ring-like enhancement pattern. This type of pathology has been rarely reported and might be based on the inflammatory nodules with central eosinophils and peripheral Langerhans cells [22]. The alternative pathology was destructive cholangitis of larger bile ducts, consequently producing the cystic-like dilatations and bile extravasations [13].

Limitations

Our study was a retrospective study with a small group of patients, so the imaging modalities and the protocols in our study were not well matched. Not all patients in this study underwent MRCP examination; thereby it remains unknown whether the stenoses of the central bile ducts were present in the other five patients. One should be cautious to make conclusions based on the specificity of these MRCP findings, because we have not compared them with other causes of sclerosing cholangitis. Further study is needed to better understand the clinical significance of these MRCP findings.

Conclusion

The stenoses of the central bile duct and the segmental dilatations and stenoses of the peripheral bile ducts on MRCP are significant characteristics in hepatic involvement of Langerhans cell histiocytosis in children. The periportal abnormal density/signal intensity and parenchymal lesions were seen on CT and MRI images in all of our patients.

Acknowledgements This work was supported by the Shanghai Municipal Public Health Bureau of the Health Administration (Grant No. 2009Y017 to Z.W.Q.); the Medical Guide Project, Shanghai Committee of Science and Technology, China (Grant No. 134119a4100 to Z.W.Q.); and Shanghai Municipal Natural Science Foundation, Shanghai Committee of Science and Technology (Grant No. 13ZR1403400 to C.M.X).

Conflicts of interest All authors claim no conflict of interest.

References

1. Schmidt S, Eich G, Geoffray A et al (2008) Extraosseous Langerhans cell histiocytosis in children. Radiographics 28:707–726, quiz 910–911
2. Weitzman S, Egeler RM (2008) Langerhans cell histiocytosis: update for the pediatrician. Curr Opin Pediatr 20:23–29
3. Schmidt S, Eich G, Hanquinet S et al (2004) Extra-osseous involvement of Langerhans' cell histiocytosis in children. Pediatr Radiol 34: 313–321
4. Abdallah M, Genereau T, Donadieu J et al (2011) Langerhans' cell histiocytosis of the liver in adults. Clin Res Hepatol Gastroenterol 35: 475–481
5. Chan YL, Li CK, Lee CY (1997) Sonographic appearance of hepatic Langerhans cell histiocytosis. Clin Radiol 52:761–763
6. Chaudhary A, Debnath J, Thulkar S et al (2006) Imaging findings in hepatic Langerhans' cell histiocytosis. Indian J Pediatr 73:1036–1038
7. Kilborn TN, Teh J, Goodman TR (2003) Paediatric manifestations of Langerhans cell histiocytosis: a review of the clinical and radiological findings. Clin Radiol 58:269–278
8. Kim M, Lyu C, Jin Y et al (1999) Langerhans' cell histiocytosis as a cause of periportal abnormal signal intensity on MRI. Abdom Imaging 24:373–377
9. Radin DR (1992) Langerhans cell histiocytosis of the liver: imaging findings. AJR Am J Roentgenol 159:63–64
10. Arakawa A, Matsukawa T, Yamashita Y et al (1994) Periportal fibrosis in Langerhans' cell histiocytosis mimicking multiple liver tumors: US, CT, and MR findings. J Comput Assist Tomogr 18:157–159
11. Wong A, Ortiz-Neira CL, Reslan WA et al (2006) Liver involvement in Langerhans cell histiocytosis. Pediatr Radiol 36:1105–1107
12. Caruso S, Miraglia R, Maruzzelli L et al (2008) Biliary wall calcification in Langerhans cell histiocytosis: report of two cases. Pediatr Radiol 38:791–794
13. Kaplan KJ, Goodman ZD, Ishak KG (1999) Liver involvement in Langerhans' cell histiocytosis: a study of nine cases. Mod Pathol 12: 370–378
14. Meyer JS, De Camargo B (1998) The role of radiology in the diagnosis and follow-up of Langerhans cell histiocytosis. Hematol Oncol Clin N Am 12:307–326
15. Jaffe R (2004) Liver involvement in the histiocytic disorders of childhood. Pediatr Dev Pathol 7:214–225
16. Ito K, Mitchell DG, Outwater EK et al (1999) Primary sclerosing cholangitis: MR imaging features. AJR Am J Roentgenol 172:1527–1533
17. Konig CW, Pfannenberg C, Trubenbach J et al (2001) MR cholangiography in the diagnosis of sclerosing cholangitis in Langerhans' cell histiocytosis. Eur Radiol 11:2516–2520
18. Siegel MJ, Herman TE (1992) Periportal low attenuation at CT in childhood. Radiology 183:685–688
19. Braier J, Ciocca M, Latella A et al (2002) Cholestasis, sclerosing cholangitis, and liver transplantation in Langerhans cell Histiocytosis. Med Pediatr Oncol 38:178–182
20. Textor HJ, Flacke S, Pauleit D et al (2002) Three-dimensional magnetic resonance cholangiopancreatography with respiratory triggering in the diagnosis of primary sclerosing cholangitis: comparison with endoscopic retrograde cholangiography. Endoscopy 34:984–990
21. Heyn RM, Hamoudi A, Newton WA Jr (1990) Pretreatment liver biopsy in 20 children with histiocytosis X: a clinicopathologic correlation. Med Pediatr Oncol 18:110–118
22. Mampaey S, Warson F, Van Hedent E et al (1999) Imaging findings in Langerhans' cell histiocytosis of the liver and the spleen in an adult. Eur Radiol 9:96–98